

Thermal Conductivity Modeling of Pure Refrigerants in a Three-Parameter Corresponding States Format¹

G. Scalabrin,^{2,3} L. Piazza,² M. Grigante,⁴ and M. Baruzzo²

The potential of the corresponding states (CS) principle for modeling a pure fluid thermal conductivity surface is studied here. While for thermodynamic properties and for viscosity, successful results have been previously obtained by directly applying an improved three-parameter CS method, significant difficulties were encountered while trying to extend this method to thermal conductivity and, in particular, it fails if applied without separately dealing with the dilute-gas term, and the residual and critical enhancement contributions. These last two parts are also combined in the excess term. It is shown that the dilute-gas term cannot be expressed in such a format, and it has necessarily to be individually modeled for each target fluid. On the contrary, the excess contribution can be described through a specific *conductivity scaling factor* that can be individually determined from a single saturated liquid conductivity experimental value. The model for the excess part is set up in a three-parameter CS format on two reference fluids, in the present case, *methane* and *R134a*, for which dedicated thermal conductivity equations are available, and it has a predictive character. The models for the dilute-gas and for the excess contributions are then combined to give the final TC model. The model has been successfully validated for two homologous families of refrigerant fluids obtaining an AAD of 3.67% for 3332 points for haloalkanes and an AAD of 2.87% for 354 points for alkanes.

KEY WORDS: alkanes; dedicated equations; halogenated alkanes; predictive model; thermal conductivity; three-parameter corresponding states; transport properties.

¹Paper presented at the Sixteenth European Conference on Thermophysical Properties, September 1–4, 2002, London, United Kingdom.

²Dipartimento di Fisica Tecnica, Università di Padova, via Venezia 1, I-35131 Padova, Italy.

³To whom correspondence should be addressed. E-mail: gscala@unipd.it

⁴Dipartimento di Ingegneria Civile Ambientale, Università di Trento, via Mesiano 77, I-38050 Trento, Italy.

1. INTRODUCTION

The development of predictive models for thermophysical properties is always regarded with great interest, particularly where the lack of reliable experimental data does not allow the development of correlative models of high accuracy. In the field of transport properties, this is specifically the case for thermal conductivity (TC) for which, due to the difficulties involved with the measurement procedures, high accuracy experimental values appeared only lately in the literature as, for example, for alkanes (A) and haloalkanes (HA).

The present work examines the corresponding states (CS) technique, specifically applied to HA, considering the increasing demand of knowledge for refrigerant fluid properties in the last few years. Apart from the specific technological interest of the new refrigerants, the approach followed in this work demonstrates the high potential of the CS principle when applied to specific families of homologous fluids. At the same time, this method provides a solution that can be extended to those fields of thermophysical properties where correlative methods fail due to the inconsistency or paucity of experimental data. Besides, it represents an alternative approach with respect to the procedure adopted to develop very precise dedicated equations, which can be followed only when a relatively large quantity of consistent experimental data are available. At the moment, this procedure has been applied to a limited number of fluids, obtaining dedicated thermal conductivity equations (DTCE) for fluids mostly belonging to A and HA. The fundamental idea of the present work consists in the utilization of these specific equations for a couple of reference fluids, associated with an original analysis of the CS method for transport properties.

The final results demonstrates that the CS principle can be applied not only to generalized thermodynamic properties but can be also used for transport properties and successfully applied to obtain innovative models.

2. CONFORMALITY ANALYSIS OF THE THERMAL CONDUCTIVITY

The extension of the CS principle to TC can be approached through a *conformality analysis* applied at first to thermodynamic properties [1]. Summarizing this concept, a group of fluids are said to be perfectly conformal if their thermodynamic surfaces $f(P_r, \rho_r, T_r) = 0$, when expressed in reduced variables, are perfectly superimposed. As it is well known, this is true only for noble gases over limited ranges of the reduced thermodynamic variables. This approach is here proposed for the TC surfaces

$f(P_r, \lambda_r, T_r) = 0$. It is worth noting that this analysis can be proposed as DTCEs are now available for a number of fluids, and they can be used to represent thermal conductivity surfaces with high accuracy. This enables verification of the degree of the *thermal conductivity conformality* and, consequently, it makes it possible to evaluate whether the CS behavior can be claimed also for this transport property function. In Figs. 1 and 2 the TC functions, presented here (for the sake of clarity) only for saturated liquid and vapor conditions, respectively, are reported as functions of the reduced temperature for a selected number of A and HA. From these figures, it can be deduced that, although for liquid conditions the $f(P_r, \lambda_r, T_r) = 0$ surfaces do not superimpose, they demonstrate a significant parallelism trend, while for the vapor phase, the behavior of the examined fluids is completely independent of each other. This analysis, simply deduced from an heuristic point of view, is sufficient to conclude that the examined fluids have, with respect to the TC, a low degree of conformality. The results of the conformality analysis for TC show a relevant different behavior with respect to that observed for thermodynamic properties [1] and for viscosity [2]. Going back to such studies, the high degree of conformality of these properties, enabled the determination of specific scaling parameters for setting up predictive and generalized models as a direct application of the CS principle.

To apply a similar procedure to TC, it has then been necessary to improve the study of the conformality behavior. The present approach

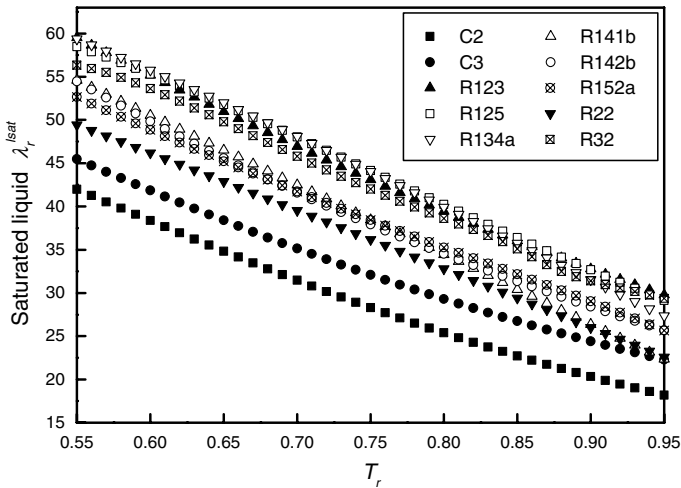


Fig. 1. Reduced thermal conductivity for saturated liquid conditions λ_r^{lsat} as a function of T_r for the studied fluids.

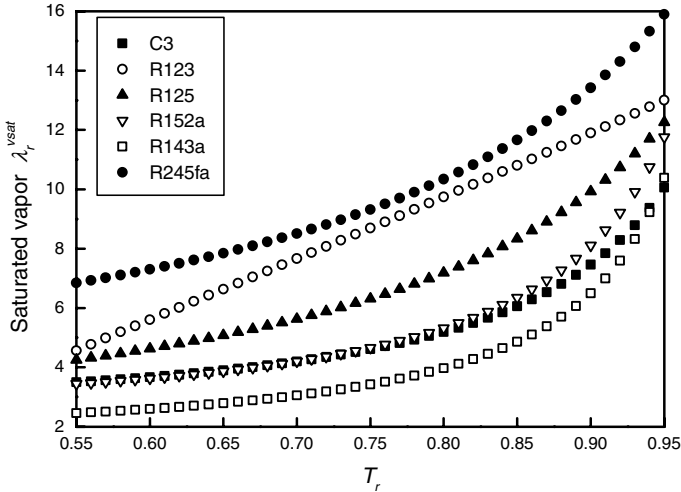


Fig. 2. Reduced thermal conductivity for saturated vapor conditions λ_r^{vsat} as a function of T_r for the studied fluids.

moves from the analysis of the correlation scheme usually assumed for the transport properties dedicated equation development. This can be seen as an equation based on the contribution of three terms depending on temperature and density:

$$\lambda(\rho, T) = \lambda_0(T) + \Delta_R\lambda(\rho, T) + \Delta_C\lambda(\rho, T) \quad (1)$$

where $\lambda_0(T)$ is the *dilute-gas* term, representing the zero-density limit of TC and depending only on temperature, $\Delta_R\lambda(\rho, T)$ is the *residual* function depending on temperature and density, whereas $\Delta_C\lambda(\rho, T)$ is the *critical enhancement* function, which is effective in a λ, ρ, T region close to the critical point.

In the former equation the last two terms are often also written as

$$\Delta_E\lambda(\rho, T) = \Delta_R\lambda(\rho, T) + \Delta_C\lambda(\rho, T) \quad (2)$$

where $\Delta_E\lambda(\rho, T)$ is designated as the *excess* term, or the additional part of TC with respect to the dilute-gas term.

To apply the CS approach in this field, it is then necessary to analyze, at first, the conformality behavior of the dilute-gas term $\lambda_0(T)$ and then of the excess contribution $\Delta_E\lambda(\rho, T)$. About the critical contribution term, it should be pointed out that, strictly close to the critical point, the

experimental TC is measured with great difficulty. To overcome this problem, a theoretical analysis has been developed to yield the critical enhancement function $\Delta_C\lambda(\rho, T)$ which is valid close to the critical point. As a consequence, the TC in such a region can be described only through critical functions specifically obtained for the fluid of interest. The modeling for this region, directly resorting to the CS approach, does not give satisfactory results. The extension of the proposed CS model to the critical region has to be presently regarded as a work in progress.

Emphasis is given here to the modeling approach followed for the dilute-gas term $\lambda_0(T)$ and the excess function representation. As the critical term $\Delta_C\lambda(\rho, T)$ is effective in a relatively wide domain near the critical region, omission of this contribution from the TC model gives rise to a significant error. It is, furthermore, necessary to point out that in a region very close to the critical point a three-parameter CS method usually cannot perform satisfactorily, also because the reference equations are not valid in such a region.

2.1. Dilute-Gas Term Analysis

In order to investigate the possibility to extend the three-parameter CS approach to the dilute-gas contribution, in Fig. 3 this term is plotted in its reduced form $\lambda_{0r}(T_r)$ vs the reduced temperature T_r for

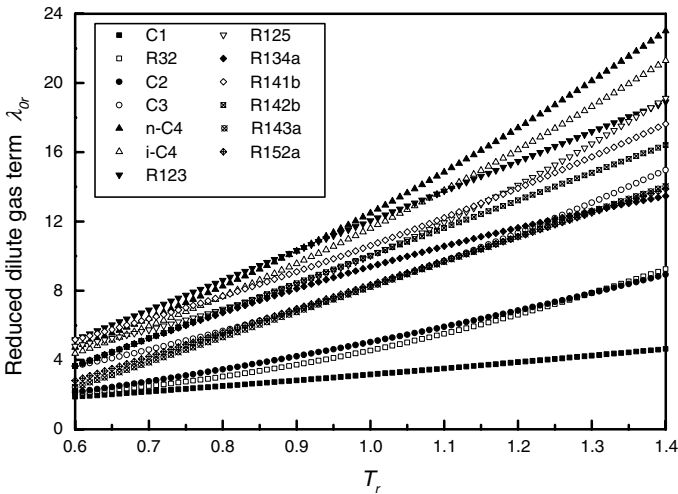


Fig. 3. Dilute-gas thermal conductivity in reduced form λ_{0r} as a function of T_r for the studied fluids.

Table I. Coefficients for the Dilute-Gas Term Equation

Fluid	Coefficients				Ref.
	<i>A</i>	<i>B</i>	<i>C</i>	<i>D</i>	
Methane	1.892461×10^{-3}	7.443056×10^{-5}	1.041690×10^{-7}	–	[3]
Ethane	–1.605872	3.312734×10^{-2}	1.471154×10^{-4}	–	[4]
Propane	2.607618	6.024197×10^{-3}	1.586886×10^{-4}	–	[5]
<i>n</i> -Butane	–	3.308681×10^{-2}	1.219902×10^{-4}	–	[6]
<i>i</i> -Butane	–4.588456	3.498096×10^{-2}	1.156719×10^{-4}	–	[7]
R22	–5.193255	4.7416636×10^{-2}	2.004695×10^{-5}	–	[8]
R32	9.430262	-5.224346×10^{-2}	2.077275×10^{-4}	–	[9]
R123 ^a	–	–	–	–	[10]
R124 ^b	–15.043	41.146	–36.294	11.192	[11]
R125	7.537477	-3.326057×10^{-2}	1.876806×10^{-4}	–	[12]
R134a	–16.57440	0.124286	-7.617690×10^{-5}	–	[13]
R141b	–	2.23430×10^{-2}	4.15420×10^{-5}	–	[14]
R142b	–12.215945	8.007880×10^{-2}	–	–	[15]
R152a	–14.94200	9.732830×10^{-2}	–	–	[16]
R143a	–13.738195	9.155812×10^{-2}	–	–	[17]
R236fa	–42.212889	0.278064	$-3.1499786 \times 10^{-4}$	–	[18]
R245fa	–2.192724	5.247022×10^{-2}	–	–	[19]
E-245mc	–11.112550	7.699999×10^{-2}	–	–	[20]

^aFor R123 the adopted relation is: $\lambda_{0r}(T) = 1000 (5.695 \times 10^{-5} T - 0.00778)$.

^bFor R124 the temperature variable is: $T^* = T/298.15$.

a selected number of fluids. The reported values originate from existing $\lambda_{0r}(T_r)$ functions, where available; alternatively, these values have been calculated from individual correlations obtained by regressing vapor TC data at very low pressure. These equations present the same temperature dependence, but they have fluid specific coefficients. The assumed functional form is

$$\lambda_{0r}(T_r) = A + B T_c T_r + C (T_c T_r)^2 + D (T_c T_r)^3 \quad (3)$$

and the coefficients are reported in Table I.

As it is well known, the critical values of the transport properties cannot be used to express the data in a reduced form; theoretically they tend to infinity. It is then necessary to introduce a pseudo-critical TC parameter K_c defined as

$$K_c = \frac{R^{5/6} P_c^{2/3}}{T_c^{1/6} M^{1/2} A^{1/3}} \quad (4)$$

where T_c is the critical temperature, P_c is the critical pressure, and M is the molar mass, while R is the universal gas constant and A is Avogadro's number. The reduced form λ_r is then obtained from

$$\lambda_r = \frac{\lambda}{K_c} \quad (5)$$

The dilute-gas correlations can be likewise expressed in a reduced form through the previous K_c factor obtaining the reduced $\lambda_{0r}(T_r)$ functions plotted in Fig. 3. This representation clearly demonstrates that the classical trend expected for quantities expressed in a CS form cannot be claimed in this case for the dilute contribution terms. Not only is a CS behavior not observed, but also these functions exhibit diverging trends. These conditions make it impossible to apply the CS principle to these terms and, consequently, it is also impossible to set up a CS modeling scheme for TC at low pressures. As a result, it is proposed to assume fluid specific correlations to represent the TC dilute-gas contribution.

2.2. Excess Term Analysis

From Eqs. (1) and (2), knowing the TC real value of $\lambda(\rho, T)$ and adopting a fluid specific expression for the dilute contribution term $\lambda_0(T)$, as those proposed in the previous section, the excess term can also be expressed as

$$\Delta_E \lambda(\rho, T) = \lambda(\rho, T) - \lambda_0(T) \quad (6)$$

Following the generalization procedure expressed by Eqs. (4) and (5), this term can be expressed in a reduced form. This quantity is plotted in Fig. 4 for saturated liquid conditions of a number of fluids. As shown by the graph, the reduced excess TC contribution does not rigorously verify the three-parameter CS criterion, because the curves do not perfectly superimpose. But, with respect to the dilute-gas contributions represented in Fig. 3, there is a strong trend for the functions to move away one from the other in a quasi-parallel mode. This finding can then be assumed as an extension of the conformality criterion for this property, demonstrating a high degree of parallelism for the TC surfaces in a CS format.

The problem is to find a property-specific scalar parameter which allows shifting from the conductivity surface of a reference fluid to one of interest. The procedure for the determination of the scalar parameters is similar to that adopted for viscosity [2] and for recent thermodynamic properties modeling [1].

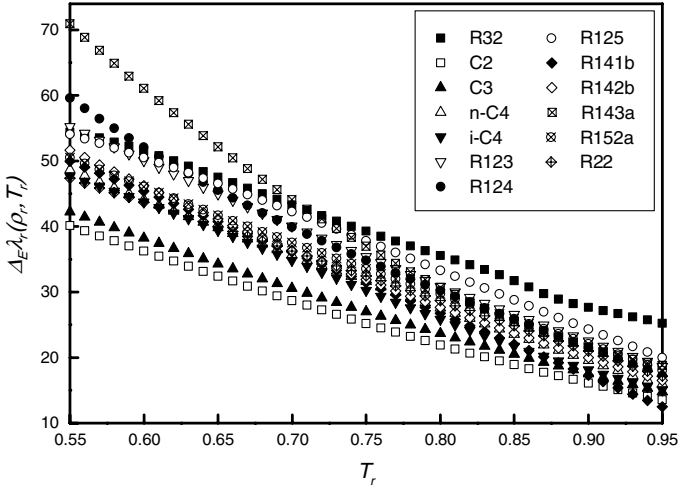


Fig. 4. Reduced excess thermal conductivity of saturated liquid $\Delta_E \lambda_r^{lsat}$ as a function of T_r for the studied fluids.

3. PROPOSED CORRESPONDING STATES MODEL FOR THERMAL CONDUCTIVITY

The first step of the model involves the definition of the *scaling parameter* suitable for TC. As a consequence of the former discussion, this parameter is specifically applied to the excess term contribution and can be simply drawn examining Fig. 4. Selecting a fluid as the reference, which in this case is methane, the individual scaling parameter κ_i can be defined as

$$\kappa_i = \left(\Delta_E \lambda_r^{lsat} \Big|_i - \Delta_E \lambda_r^{lsat} \Big|_{ref} \right)_{T_r} \quad (7)$$

where $\Delta_E \lambda_r^{lsat} \Big|_i$ is the reduced excess TC of the fluid of interest at saturated liquid conditions and $\Delta_E \lambda_r^{lsat} \Big|_{ref}$ is the corresponding quantity of the reference fluid. The subscripts E and r stand for *excess* and *reduced*, respectively, whereas the superscript *lsat* stands for the saturated liquid condition. For the target fluid the $\Delta_E \lambda_r^{lsat} \Big|_i$ value is obtained from an experimental saturated liquid value, at a selected T_r , through Eq. (6) in which the dilute term has to be known, as from the general assumptions of the model. The $\Delta_E \lambda_r^{lsat} \Big|_{ref}$ term is instead calculated from the TCDE of methane, as the reference fluid.

As a general rule, the κ_i values can be defined at a generic reduced temperature T_r . The only criterion limiting this choice is the availability

of experimental data or individual correlations for the saturated liquid condition. For the studied fluids, most of the TC saturated liquid data bracket the range $0.7 \leq T_r \leq 0.8$. To avoid extrapolation and in order to refer the scalar parameters to actual experimental values, the selection of $T_r = 0.75$ looks to be the best compromise to fulfil these conditions.

For the case that the κ_i scaling factor can be considered in a range of T_r as independent from T_r and that the $\Delta_E \lambda_r^{\text{lsat}}(T_r)|_{\text{ref}}$ function is known, any other $\Delta_E \lambda_r^{\text{lsat}}(T_r)|_i$ function can be obtained from linear scaling through κ_i . Because for conformal fluids at each T_r the saturated liquid thermal conductivity vs κ_i tends to fall on a straight line, as shown in Fig. 4, the saturated liquid thermal conductivity of a target fluid can be obtained through interpolation, by means of κ_i , of the thermal conductivity of two reference fluids at the same T_r . Assuming that the same linear scaling is constant away from the saturated liquid condition, that is, for the liquid, vapor, and supercritical regions, namely

$$\kappa_i(T_r, P_r)|_{\substack{\text{liq} \\ \text{vap} \\ \text{scrit}}} = \kappa_i|_{T_r}^{\text{sl}} = \text{const} \tag{8}$$

the former results can be extended to the entire $\lambda_r T_r P_r$ surface. After determining these values for the homologous families of fluids investigated here, a CS model for the *excess term* can then be set up in a classical three-parameter CS format as follows.

Two fluids of the family have to be chosen as references. At given T , P values of the fluid of interest, the densities of the two reference fluids have to be calculated at the same reduced conditions, T_r and P_r , of the fluid of interest by their dedicated equation of state implicitly solved in the density variable:

$$\begin{cases} P_r = P_r^{r1}(T_r, \rho_r^{r1}) \\ P_r = P_r^{r2}(T_r, \rho_r^{r2}) \end{cases} \tag{9}$$

where superscripts r1 and r2 stand for the reference fluids. These density values are used as input variables, together with T_r , to calculate the corresponding TC values of the reference fluids, $\lambda^{r1}(\rho^{r1}, T^{r1})$ and $\lambda^{r2}(\rho^{r2}, T^{r2})$, respectively, through their DTCEs, where for r1 it is $T^{r1} = T_r T_c^{r1}$ and similarly for r2. Subtracting from these values the dilute-gas contributions, $\lambda_0^{r1}(T^{r1})$ and $\lambda_0^{r2}(T^{r2})$ for the references r1 and r2, respectively, the obtained values represent the excess contributions $\Delta_E \lambda^{r1}(\rho^{r1}, T^{r1})$ and $\Delta_E \lambda^{r2}(\rho^{r2}, T^{r2})$ of the reference fluids. According to the former procedure, Eqs. (4) and (5), the reduced forms of the excess contributions are

$$\begin{aligned}\Delta_E \lambda_T^{r1} &= \frac{\Delta_E \lambda^{r1}(T^{r1}, \rho^{r1})}{K_c^{r1}} \\ \Delta_E \lambda_T^{r2} &= \frac{\Delta_E \lambda^{r2}(T^{r2}, \rho^{r2})}{K_c^{r2}}\end{aligned}\quad (10)$$

From these values and the κ_i value of the target fluid, its excess contribution $\Delta_E \lambda_r(T_r, \rho_r)$ can be determined in reduced form by solving the three-parameter CS equation:

$$\Delta_E \lambda_r(T_r, \rho_r, \kappa_i) = \Delta_E \lambda_r^{r1} + \frac{\kappa_i - \kappa^{r1}}{\kappa^{r2} - \kappa^{r1}} \left(\Delta_E \lambda_r^{r2} - \Delta_E \lambda_r^{r1} \right) \quad (11)$$

The excess term of the fluid can then be obtained as a function of temperature and density by

$$\Delta_E \lambda(\rho, T)_i = K_{ci} \Delta_E \lambda_r(T_r, \rho_r, \kappa_i) \quad (12)$$

and, given the dilute-gas term $\lambda_0(T)_i$ of the fluid of interest, its overall λ can be determined as

$$\lambda(\rho, T)_i = \lambda_0(T)_i + \Delta_E \lambda(\rho, T)_i \quad (13)$$

For the fluid of interest, besides the individual dilute-gas term $\lambda_0(T)$, the only specific parameters required are then T_c , P_c and a single TC experimental value for the saturated liquid at $T_r = 0.75$ from which to obtain $\Delta_E \lambda_r^{\text{sat}}|_i$ from Eq. (6) and then κ_i from Eq. (7). In Table II, the κ_i values calculated from data of the cited references are reported together with the assumed critical parameters for the investigated fluids.

3.1. Choice of the Reference Fluids

For the proposed model, the choice of the reference fluids influences the results and determines the ranges of application of the model. At first, the selected reference fluids have to fulfil some requirements:

1. Availability of a dedicated equation of state in order to ensure high accuracy for the required conversion from the T, P to the T, ρ variables.
2. Availability of an accurate TC equation with a wide range of validity in the T_r and P_r domain.
3. The TC equations of the reference fluids need to have the critical enhancement term. In the proposed model, a domain very close to the critical region has not been considered; the critical enhancement contribution of the reference equations can be used

Table II. Critical Data and Fundamental Parameters for the Proposed Model. (Methane is the reference fluid for the parameter κ_i calculation)

Fluid	Formula	T_c (K)	P_c (MPa)	M	κ_i	Ref.
<i>Halogenated alkanes</i>						
R22	CHF ₂ Cl	369.29	4.988	86.469	12.5633	[9]
R32	CH ₂ F ₂	351.25	5.782	52.024	19.2621	[12]
R123	CHCl ₂ CF ₃	456.83	3.668	152.930	15.4515	[13]
R125	CHF ₂ CF ₃	339.33	3.629	120.022	17.9330	[14]
R134a	CH ₂ FCF ₃	374.18	4.056	102.032	18.1325	[15]
R141b	CFCl ₂ CH ₃	477.35	4.190	116.940	11.5346	[16]
R142b	CF ₂ ClCH ₃	410.25	4.123	100.496	11.9805	[21]
R152a	CH ₃ CHF ₂	386.41	4.495	66.051	13.6459	[22]
R124	CHClCF ₄	395.42	3.636	136.480	14.9165	[23]
R143a	CF ₃ CH ₃	346.04	3.780	84.048	17.0477	[24]
R236fa	1,1,1,3,3,3-hexafluoropropane	398.07	3.200	152.040	31.0674	[18]
R245fa	1,1,1,3,3-pentafluoropropane	430.75	3.640	134.050	20.9666	[19]
E-245mc	CF ₃ CF ₂ OCH ₃	406.83	2.887	150.054	41.6953	[25]
<i>Alkanes</i>						
Methane	CH ₄	190.56	4.599	16.0428	^a	[4]
Ethane	C ₂ H ₆	305.33	4.872	30.07	5.2894	[7]
Propane	C ₃ H ₈	369.85	4.247	44.098	7.0779	[6]
<i>n</i> -Butane	<i>n</i> -C ₄ H ₁₀	425.16	3.796	58.125	11.6846	[6]
<i>i</i> -Butane	<i>iso</i> -C ₄ H ₁₀	407.85	3.640	58.125	10.3124	[7]

^aReference fluid.

to account for possible influences of the critical behavior outside that domain.

4. Because for most of the fluids the dilute-gas terms have been obtained from experimental data regression, their T_f validity domains are different for each fluid and, in some cases, very limited. As a consequence, the selection criterion imposes that the dilute-gas terms of the reference fluids bracket the corresponding terms of the target fluids.

After a detailed analysis of the TC surfaces and according to the examined constraints, the fluids selected as references were *methane* and *R134a*. For sake of brevity, detailed information on their equations are omitted here and reference is made to the original publications for methane [26] and for *R134a* [27]. This choice has the advantage to set up a single model, based on the same reference fluids, which can be used to represent the TC surfaces of both A and HA. Taking into account the validity ranges of the reference equations, the model is applicable in

the temperature ranges $0.734 \leq T_r \leq 0.99$ below the critical isotherm and $1.01 \leq T_r \leq 1.095$ above the critical isotherm, whereas the pressure range is up to $P_r = 17.258$. As discussed earlier, the use of DTCEs including a critical enhancement term enables the extension the model validation close to the critical point.

As the model accuracy depends on that of the reference DTCEs, validation of these equations needs to be done. The available data, inside the validity range of the equations, have been divided into different regions, and the results are reported in Table III.

For *methane*, the number of sources is limited and the saturated conditions cannot be tested, but for the available data the accuracy is high, with less reliable results in the near-critical region with data from a single source. The performance of the *R134a* DTCE is good over the whole surface with less reliable results for the vapor phase. The overall AAD values of both reference equations are less than the normal experimental uncertainties, and the bias values are excellent for both fluids demonstrating the absence of shifting of these DTCEs.

Equation (11) can also be incidentally applied for a preliminary test checking the conformality of a fluid of interest with respect to a family of fluids for which a couple of references are already known. Comparison of the few available data of such a fluid with the corresponding values predicted by that equation, allows verification of the conformality degree of the fluid.

4. MODEL VALIDATION AND DISCUSSION OF RESULTS

Some preliminary considerations can be drawn for the validation. At first, most of the available experimental measurements are limited to the *halogenated alkanes* and *alkanes* considered here. Comparing the quality of the existing data sets, it clearly emerges that their experimental uncertainty stands around 3 to 4% and these results represent reference values for the accuracy of any CS model for TC; this is also the accuracy level of the available DTCEs.

Besides the limited availability of data, there are two other reasons to focus the present study to these two families. The first is that the effectiveness of the CS principle is highly improved if applied to homologous families such as these ones. The second is that testing the model both on regular fluids as the alkanes and on polar fluids as the haloalkanes is an important challenge for the model validation.

The validity ranges of the reference fluid dedicated equations limit the model range which then restrains the number of experimental data to use for validation. For this reason in Tables IV and V the data inside

Table III. Validation Results of the Methane and R134a DTCE's Selected as Reference Fluids^a

Phase	Range <i>P</i> (MPa)	Range <i>T</i> (K)	NPT		AAD (%)	Bias (%)	Max (%)	Ref
			NPT	Inside model range				
<i>Methane</i>								
l	2.583–70.083	140.07–320.07	188	127	1.474	0.990	9.793	[28]
l	0.357–69.419	144.02–312.21	225	210	0.879	–0.493	71.40	[29]
v	0.103–0.103	140.49–324.00	18	12	2.203	–2.203	2.853	[30]
v	1.864–6.130	323.15–325.15	15	4	0.889	0.640	1.538	[31]
v	0.101–20.610	314.26–314.26	12	12	1.467	–1.467	2.963	[28]
v	0.101–19.292	325–93–325–93	14	14	1.037	–0.947	2.246	[32]
v	0.101–78.500	298.45–307.35	193	31	1.370	–1.370	2.834	[33]
v	0.101–0.101	323.15–32.15	5	1	1.395	1.395	1.395	[28]
sc	0.116–33.866	277.59–310.92	25	10	3.439	3.086	5.835	[34]
Overall			695	421	1.218	–0.120	71.4069	
<i>R134a</i>								
l	0.135–6.097	253.25–363.15	46	46	3.024	–3.024	8.040	[3]
l	0.622–26.169	249.24–292.29	293	189	1.119	1.091	2.217	[35]
l	0.752–5.962	301.07–371.65	547	547	2.060	–1.079	6.957	[35]
l	2.000–50.000	299.18–399.22	243	243	1.926	0.968	31.353	[36]
l	0.964–45.480	302.04–349.38	150	84	0.685	–0.273	1.417	[36]
l	1.318–5.177	240.87–303.04	48	32	0.708	0.103	1.583	[9]
sl	0.693–0.697	301.26–303.27	28	28	1.125	–1.125	2.347	[6]
sl	0.091–0.519	290.06–244.92	19	8	0.600	0.419	2.374	[6]
sl	0.075–0.702	240.00–300.00	21	13	2.838	2.838	4.004	[37]
sv	0.132–2.625	253.10–353.00	38	38	7.215	7.215	18.570	[37]
v	0.130–1.300	272.99–333.45	19	19	1.710	1.710	3.012	[38]
v	0.096–2.585	273.75–354.15	42	42	1.976	–1.304	5.766	[3]
v	0.100–0.100	303.00–383.00	5	3	2.092	0.346	2.618	[39]
v	0.102–0.974	301.22–391.27	338	239	3.707	–1.087	13.127	[35]
v	0.021–1.743	241.21–341.78	417	417	5.646	5.391	24.234	[35]
v	0.102–3.487	301.48–373.35	944	944	3.584	1.857	9.626	[35]
v	0.101–0.101	299.18–405.82	32	15	3.201	0.742	4.825	[36]
v	0.101–0.101	299.18–405.82	27	15	3.159	–0.700	3.843	[40]
v	0.101–0.101	303.15–343.15	5	5	3.887	–3.887	6.326	[5]
v	0.100–0.100	298.15–343.15	6	6	3.827	–3.827	6.481	[40]
v	0.027–0.030	294.50–363.20	8	8	1.355	1.025	3.407	[41]
v	0.100–0.100	250.00–400.00	9	9	0.772	–0.105	1.626	[42]
v	0.050–0.200	235.33–439.51	21	16	1.878	0.795	3.863	[42]
v	0.100–3.050	273.15–363.15	38	38	7.215	7.215	18.57	[43]
Overall			3344	3004	3.278	–0.097	31.353	

^aPhase: l = liquid, sl = saturated liquid, v = vapor, sv = saturated vapor, sc = supercritical.

and outside the model range have been designated as “*inside model range*” and “*outside model range*”, respectively, but the analysis of the validation results obviously pertains only to the data inside the model range. It is important to stress that no preliminary screening of the used data has been done and that the obtained accuracy is then directly related to the experimental uncertainty. This can be seen, for instance, by observing the results of the different experimental data sets tested against DTCEs specifically for R123 and R152a. However, the fluids for which these equations are available with a complete formulation including the critical enhancement are very few: R123, R152a, and R134a among HAs, and methane and ethane among As. R134a and methane, being used as references, have been validated separately. For this reason the comparison of the present model with DTCEs of refrigerants is so limited.

4.1. Validation for Haloalkanes

Together with the model results, Table IV reports also the experimental data sources presently available for HAs, fluoropropanes (FP), and a fluoroether (FE). The data for R123, R152a, R142b, R22, R124, R141b, R143a, R125, and R32 comprise a total of 5598 points, but considering the model validity range, a total of 3106 experimental points have been used. For the FPs R245fa and R236fa and the FE, the total data are 318, of which 226 are here examined. In spite of the limited number of TC data, the available sources span liquid, vapor, and supercritical regions, in addition to saturation conditions. For this reason, the obtained results have been separately reported according to their phases.

4.1.1. Liquid Region

For all the fluids the proposed model attains results of good accuracy and comparable with that claimed for experimental measurements. For those fluids with a significant number of sources, the results in terms of AAD (Absolute Average Deviation) are within 2 to 3%. These results are confirmed, in particular, for R123 and R152a, which is comparable with the corresponding performances of the dedicated equations. Not only is the overall AAD practically the same between the two, with similar bias levels for each of the sources, but also the least reliable results correspond to the same sources, as, for example, the R152a liquid data set of Ref. 56, for which the bias value confirms an evident shifting of data.

In Fig. 5, the deviations of the model for a number of HAs are plotted as a function of reduced temperature, and they are confined within a $\pm 4\%$ error band. The results for three polar fluids with six different data sources are represented by the model without any significant trend in the

Table IV. Model Validation for Halogenated Alkanes

Phase ^a	Range <i>P</i> (MPa)	Range <i>T</i> (K)	NPT	NPT mod. range	This model			Dedicated equation			Ref.
					AAD (%)	Bias (%)	Max (%)	AAD (%)	Bias (%)	Max (%)	
<i>R123</i>											
l	0.38-6.13	343.5-353.9	42	8	0.294	-0.040	0.826	0.533	-0.533	1.412	[3]
l	1.00-30.0	353.3-353.4	36	4	0.659	0.659	0.872	0.383	0.383	0.539	[44]
sv	0.39-0.64	344.2-364.3	6	2	8.030	-8.030	8.521	8.278	-8.278	8.984	[45]
v	0.34-0.50	344.2-364.3	6	2	9.353	-9.353	9.659	9.332	-9.332	9.353	[45]
v	0.10-0.59	344.2-364.5	32	18	5.542	-5.542	7.351	5.370	-5.370	7.707	[3]
v	0.10-0.25	343.0-463.0	8	6	0.400	0.279	0.605	0.702	0.702	0.971	[4]
v	0.10-0.72	353.2-373.2	13	9	3.780	-3.780	5.270	3.402	-3.402	5.077	[46]
l	0.10-23.80	253.3-333.3	36	0	Outside model range			-	-	-	[47]
l	0.10-200.0	283.1-323.1	36	0	Outside model range			-	-	-	[7]
l	0.38-16.4	212.1-302.6	66	0	Outside model range			-	-	-	[48]
sl	0.00-0.07	173.3-291.3	17	0	Outside model range			-	-	-	[6]
sl	0.01-0.28	253.1-333.1	5	0	Outside model range			-	-	-	[47]
sv	0.12-0.25	306.1-328.1	6	0	Outside model range			-	-	-	[5]
v	0.03-0.12	288.6-322.0	124	0	Outside model range			-	-	-	[49]
Overall			433	49	3.589	-3.358	9.659	3.520	-3.458	9.353	
<i>R152a</i>											
l	0.51-6.22	292.9-363.2	44	28	0.923	0.787	1.369	0.775	0.372	1.264	[43]
l	2.79-17.9	293.6-293.6	38	6	1.501	1.501	2.042	1.087	1.087	1.780	[50]
l	0.78-20.0	294.2-398.5	78	78	1.586	0.733	4.179	3.009	2.948	6.611	[51]
l	2.10-20.1	298.2-323.2	25	10	1.480	-1.480	4.200	1.095	-1.095	2.379	[52]
l	7.89-7.89	299.8-385.2	11	1	2.065	-2.065	2.065	2.165	-2.165	2.165	[53]
l	1.60-30.6	303.6-342.6	20	12	1.731	1.697	4.093	2.617	2.548	6.055	[54]
l	2.79-17.9	292.6-294.3	38	6	1.471	1.471	2.075	1.059	-1.059	1.638	[55]
l	3.09-9.35	367.2-367.2	31	6	11.93	-11.93	18.92	7.223	-7.091	14.915	[56]

Table IV. (Continued)

Phase ^a	Range <i>P</i> (MPa)	Range <i>T</i> (K)	NPT	NPT inside mod. range	This model			Dedicated equation			Ref.
					AAD (%)	Bias (%)	Max (%)	AAD (%)	Bias (%)	Max (%)	
l	0.50–4.14	293.2–382.1	47	27	9.732	-9.732	15.922	7.322	-7.322	11.390	[56]
l	0.98–22.4	293.2–332.9	37	23	1.493	-1.493	3.425	0.998	-0.998	1.716	[57]
l	1.00–55.0	307.4–378.2	247	247	3.603	-3.603	11.420	2.616	-2.616	8.626	[58]
sl	0.52–4.40	293.6–385.0	5	1	1.026	1.026	1.026	1.047	1.047	1.047	[50]
sl	0.59–1.18	298.1–323.2	5	2	3.235	-3.235	4.850	2.130	-2.130	2.887	[52]
sl	0.44–4.45	288.7–385.7	16	11	2.315	-2.197	5.433	1.712	-0.059	6.634	[59]
sl	0.51–1.50	293.1–333.2	5	3	2.132	-2.132	3.519	0.756	-0.756	1.023	[57]
sv	2.70–4.45	360.1–385.8	4	4	0.672	0.667	1.807	6.869	-6.869	9.205	[59]
v	0.10–0.10	300.0–420.0	13	7	0.923	0.787	1.369	0.775	0.372	1.264	[43]
v	0.08–2.253	293.9–353.8	40	36	1.535	0.835	3.584	2.051	-0.463	5.513	[52]
v	0.10–0.10	303.0–423.0	5	4	2.551	-1.867	5.138	2.846	-2.279	5.517	[4]
v	0.10–0.10	288.4–349.0	14	13	9.937	9.937	12.243	9.179	9.179	11.825	[8]
v	2.23–3.09	367.1–367.1	25	5	2.410	2.188	5.044	2.563	-2.090	3.800	[56]
v	2.09–3.76	348.2–376.9	30	8	7.566	7.566	13.139	4.287	-0.142	11.027	[56]
v	0.10	298.4–455.6	28	24	3.028	2.140	11.605	2.881	1.757	10.695	[58]
sc	6.00–41.0	390.9–455.6	127	36	7.198	-7.198	11.637	3.183	-3.183	7.009	[58]
	Overall		933	602	3.506	-1.945	15.922	2.855	-1.118	14.915	
<i>R/42b</i>											
l	2.10–20.1	323.1–323.2	25	5	1.208	1.280	1.666				[52]
l	1.46–69.6	302.2–304.3	64	64	1.635	-1.629	4.498				[9]
l	0.99–17.1	330.0–403.0	41	25	1.575	1.136	3.189				[10]
l	1.20–30.3	312.5–332.7	24	8	1.961	1.961	2.936				[54]
sl	0.68–0.68	323.1–32.15	5	1	0.826	0.826	0.826				[52]
sl	0.82–1.92	330.0–368.0	5	2	1.176	1.176	2.145				[10]
v	0.10–0.10	320.0–440.0	12	7	3.080	-3.080	5.723				[43]

v	0.10-0.10	318.0-418.0	5	4	2.355	-2.355	4.431	[39]
v	0.37-3.50	330.0-403.0	15	15	5.894	5.880	8.609	[10]
v	0.10-1.35	313.2353.2	21	18	9.152	9.152	13.745	[12]
sc	0.39-20.4	400.0-444.37	121	108	5.364	-3.214	26.340	[10]
	Overall		338	257	3.842	-0.683	26.340	
R22								
l	1.00-26.5	273.1-333.2	37	30	1.324	-1.231	3.064	[47]
l	2.10-20.1	273.1-323.2	25	15	1.408	-1.347	2.584	[52]
l	0.90-0.09	274.5-289.6	16	5	0.635	0.033	1.455	[53]
l	1.07-55.0	299.1-356.6	288	288	2.774	-2.737	10.229	[11]
sl	0.49-2.42	273.2-333.2	5	4	2.745	-2.600	5.904	[47]
sl	0.49-1.94	273.1-323.1	5	3	1.439	-1.316	3.102	[52]
sl	0.53-3.75	275.1-54.4	6	4	3.222	-3.222	5.844	[21]
v	0.10-0.10	289.5-346.8	4	4	11.319	7.151	36.941	[13]
v	0.10-0.10	303.0-383.0	5	3	1.990	1.990	2.145	[4]
v	0.10-5.76	298.1-393.1	131	131	2.783	0.151	6.258	[14]
v	0.01-0.01	294.9-373.4	34	34	0.999	0.274	2.669	[15]
v	0.10-0.10	278.2-401.35	15	8	1.171	-0.043	2.543	[16]
v	0.10-0.10	295.0-385.9	24	17	4.129	1.596	8.603	[11]
sc	7.00-46.0	375.6-393.9	318	72	7.350	-7.350	11.59	[11]
	Overall		913	618	3.141	-2.119	36.941	
R124								
l	0.63-18.2	293.1-333.1	35	21	0.623	0.002	1.313	[22]
l	0.80-30.5	294.7-353.8	25	17	1.485	0.602	2.454	[60]
l	0.38-2.07	298.5-366.2	9	4	0.780	-0.780	1.575	[61]
sl	0.32-0.99	293.2-333.2	5	3	0.339	0.114	0.382	[22]
v	0.13-0.59	293.4-333.2	12	11	3.578	3.578	5.052	[38]
	Overall		86	56	1.461	0.836	5.052	

Table IV. (Continued)

Phase ^a	Range <i>P</i> (MPa)	Range <i>T</i> (K)	NPT	NPT inside mod. range	This model			Dedicated equation			Ref.
					AAD (%)	Bias (%)	Max (%)	AAD (%)	Bias (%)	Max (%)	
<i>R/41b</i>											
l	0.70–30.4	353.1–392.1	29	9	4.109	4.109	6.494	4.109	4.109	6.494	[54]
v	0.10–0.10	353.1–392.1	4	1	8.641	8.641	8.641	8.641	8.641	8.641	[12]
l	0.27–21.7	253.1–333.1	28	0		Outside model range					[22]
l	0.45–16.4	209.1–246.1	48	0		Outside model range					[48]
sl	0.01–0.25	253.1–333.1	5	0		Outside model range					[22]
sl	0.01–0.10	248.6–303.9	6	0		Outside model range					[62]
v	0.05–0.25	284.1–333.1	6	0		Outside model range					[5]
v	0.02–0.14	281.0–332.5	87	0		Outside model range					[49]
v	0.1	284.1–333.1	3	0		Outside model range					[23]
	Overall		216	10	4.562	4.562	8.641	4.562	4.562	8.641	
<i>R/43a</i>											
l	2.00–20.0	272.4–323.4	23	14	9.609	9.609	12.352	9.609	9.609	12.352	[56]
l	2.48–50.0	316.9–336.9	93	93	1.993	1.473	4.448	1.993	1.473	4.448	[63]
l	3.00–48.0	304.7–305.7	49	49	3.746	3.746	4.719	3.746	3.746	4.719	[63]
sl	0.62–3.40	273.1–341.1	16	16	3.296	1.021	7.046	3.296	1.021	7.046	[64]
sv	2.06–3.37	318.12–341.1	10	10	3.810	2.095	7.347	3.810	2.095	7.347	[64]
v	0.10–0.10	298.0–343.0	5	3	11.479	-11.479	12.630	11.479	-11.479	12.630	[39]
v	0.03–0.30	272.7–323.7	190	190	1.133	0.203	8.169	1.133	0.203	8.169	[49]
v	0.54–1.39	304.4–307.1	19	19	3.358	3.358	5.545	3.358	3.358	5.545	[63]
v	0.10–0.10	299.2–377.3	32	24	1.996	-1.804	4.850	1.996	-1.804	4.850	[63]
sc	0.10–45.0	374.2–377.3	92	56	4.517	-4.517	9.191	4.517	-4.517	9.191	[63]
sc	0.10–45.0	374.2–377.3	336	0		Outside model range					[63]
	Overall		865	474	2.549	0.557	12.630	2.549	0.557	12.630	

Table IV. (Continued)

Phase ^a	Range <i>P</i> (MPa)	Range <i>T</i> (K)	NPT	NPT inside mod. range	This model			Dedicated equation			Ref.
					AAD (%)	Bias (%)	Max (%)	AAD (%)	Bias (%)	Max (%)	
v	0.10-0.50	299.2-299.2	2	2	2.109	2.109	2.574				[73]
sc	0.10-0.50	361.8-384.9	131	66	9.876	-9.797	15.877				[73]
sc	0.10-0.50	361.8-384.9	203	0	Outside model range						[73]
Overall			659	371	6.018	-5.500					
<i>R245fa</i>											
sl	0.51-1.81	336.9-390.4	14	6	4.122	-4.122	7.732				[17]
v	0.10-2.50	346.7-413.6	26	22	2.024	-1.946	4.329				[17]
v	0.10-0.10	333.2-382.2	4	4	10.551	-10.551	15.373				[17]
sv	0.35-2.69	323.2-410.4	10	8	4.133	1.378	11.162				[23]
l	0.70-14.7	253.4-314.9	16	0	Outside model range						[24]
Overall			70	40	3.613	-2.468	15.373				
<i>R236fa</i>											
sl	0.42-2.08	312.5-377.2	13	7	9.517	-9.517	12.420				[17]
v	0.03-0.52	301.4-342.8	169	144	1.396	-0.097	4.621				[17]
v	0.10-0.10	315.2-414.6	10	6	9.517	-9.517	15.42				[17]
Overall			192	157	2.071	-0.877	12.420				
<i>E245mc</i>											
sl	0.22-0.45	300.0-323.2	8	4	0.838	0.838	1.414				[74]
l	1.0	275.2-323.6	11	6	0.741	0.677	1.296				[74]
l	2.1-10.0	283.2-323.2	23	5	0.610	0.507	1.193				[74]
v	0.05-0.23	303.2-323.2	14	14	2.686	-2.667	6.529				[20]
Overall			56	29	1.671	-0.944	6.529				
Overall haloalkanes				3332			3.674				

^aPhase: l = liquid, sl = saturated liquid, v = vapor, sv = saturated vapor, sc = supercritical.

Table V. Model Validation for Alkanes

Phase ^a	Range <i>P</i> (MPa)	Range <i>T</i> (K)	NPT	NPT inside mod. range	AAD (%) Bias (%) Max (%)			Ref.
					This model			
Ethane								
l	0.11–34.7	277.6–310.9	28	12	3.134	3.134	5.589	[75]
l	0.10–78.5	306.5–309.3	113	15	1.584	–0.475	3.024	[33]
v	0.99–3.99	325.0–325.0	5	5	1.611	–1.611	2.587	[31]
v	0.10–19.8	315.1–329.8	79	67	2.932	0.747	13.976	[32]
sc	1.94–17.2	33.1–33.2	11	11	2.760	–1.881	8.752	[76]
v	0.10–19.6	41.9–67.2	13	0	Outside model range			[77]
	Overall		249	110	2.692	0.471		
Propane								
l	1.58–67.5	296.2–301.4	400	68	0.920	–0.284	2.043	[78]
l	5.61–34.6	277.6–377.6	24	18	4.152	3.663	10.145	[79]
l	1.87–27.7	323.2–360.4	40	40	1.977	0.594	7.848	[80]
l	3.22–67.5	298.3–299.5	70	10	0.921	–0.473	1.738	[81]
l	1.50–29.9	274.2–315.7	16	12	0.875	0.699	1.465	[82]
sl	1.65–4.25	322.0–369.8	7	7	2.290	0.547	4.092	[80]
v	0.12–4.18	277.6–377.6	9	7	5.413	5.413	14.137	[79]
v	0.10–3.12	323.2–360.4	11	11	2.787	0.282	7.524	[80]
v	0.10–0.10	323.2–398.2	5	4	0.626	0.235	1.665	[83]
sv	1.65–4.25	322.0–369.8	7	7	9.060	9.060	14.884	[79]
sc	0.10–28.5	378.7–369.2	32	19	7.493	–2.228	39.023	[80]
l	0.10	93.1–223.1	14	0	Outside model range			[84]
	Overall		635	203	2.605	0.464		
<i>n</i>-Butane								
l	0.80–20.0	316.0–335.6	15	6	0.490	–0.517	0.900	[18]
l	0.11–36.7	344.3–444.3	45	30	5.868	5.391	10.341	[85]
v	0.10–0.10	323.2–423.1	5	5	2.619	2.619	3.485	[86]
l	0.10	143.1–272.6	14	0	Outside model range			[84]
sl	0.00–0.04	148.2–252.2	36	0	Outside model range			[87]
	Overall		115	41	4.684	4.188		
Overall alkanes				354	2.873	0.898		

^aPhase: l = liquid, sl = saturated liquid, v = vapor, sv = saturated vapor, sc = supercritical.

error deviation, showing that the existing scatter is largely dependent on the experimental uncertainty of the data.

4.1.2. Saturation Conditions

The former comments for the liquid phase results can be likewise extended to those at coexistence conditions, and specifically for the saturated liquid. On the other hand, for the saturated vapor the data are so limited that conclusions cannot be drawn.

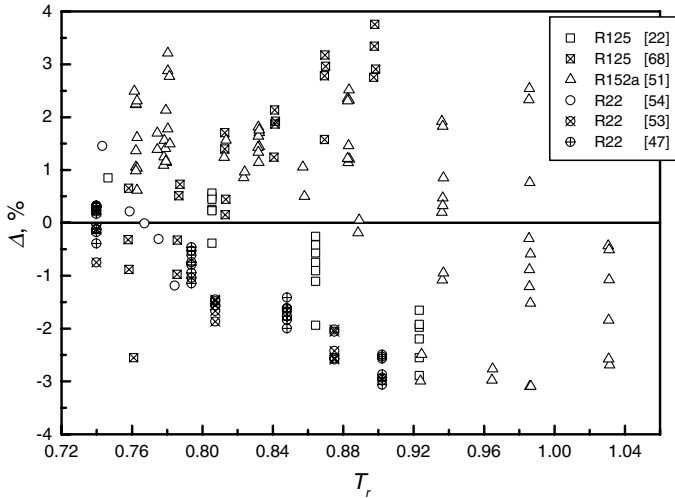


Fig. 5. Thermal conductivity deviations of pure fluids in the liquid region as a function of T_r .

4.1.3. Vapor and Supercritical Regions

The model performance shows very interesting results in this case too. Worse results are obtained for supercritical conditions, evidently because the model cannot properly account for the critical enhancement contribution. In the vapor phase, the model performs very well with an accuracy level similar to that of the dedicated equations as in the case of R123 and R152a. Excluding some references with a marked bias, such as Ref. 13 for R22 and Ref. 39 for R143a, the results for these conditions are also within the experimental uncertainty. Considering that the scaling parameters are calculated at saturated liquid conditions, the results obtained for the vapor phase demonstrate the high potential of the CS model approach.

In Fig. 6, the deviations are now plotted as a function of T_r for the same group of HAs formerly examined for the liquid. In this case, the deviations are confined in a $\pm 10\%$ error band which is more than twice the span for the liquid region. Also, in this case the data are represented without an evident bias.

Summarizing the results, the overall AAD obtained for all the 3332 points of the HAs and FPs is 3.67% which is comparable with the average value of the claimed experimental uncertainty and demonstrates the high accuracy of the model.

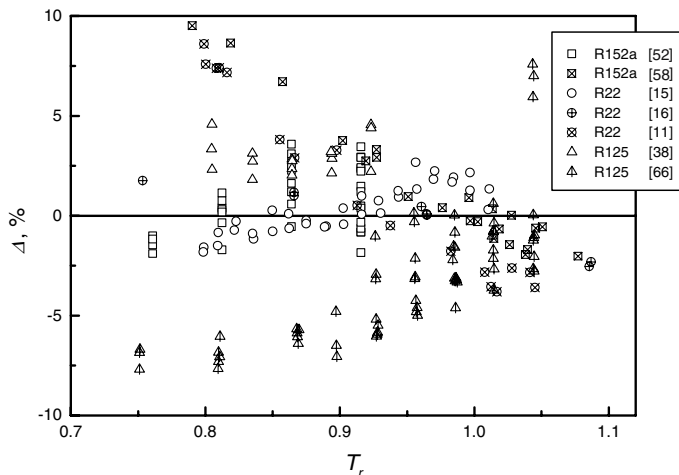


Fig. 6. Thermal conductivity deviations of pure fluids in the vapor region as a function of T_r .

4.2. Validation for Alkanes

For this family of fluids it is more difficult to sum up a general performance of the model because of the limited amount of available data sources. Excluding methane used as a reference component, only propane provides a significant number of experimental values as shown on Table V. Apart from the data sets pertaining to the saturated vapor and supercritical regions, the results obtained for propane in the other regions are similar to those reached for HAs and the results for ethane are of a similar level. Considering all the regions, the overall AAD for a total of 354 points for ethane, propane, and *n*-butane is 2.87%, exhibiting a high accuracy level also for these fluids.

5. CONCLUSIONS

Through an innovative analysis the potential of the CS principle is examined to extend to TC the three-parameter modeling techniques recently implemented for thermodynamic properties and viscosity. The proposed method extends the classical concept of CS conformality to TC and defines for this quantity a new fluid-specific scaling parameter of high effectiveness for the development of predictive schemes. A single experimental value of the saturated liquid TC is required to calculate such a scaling parameter. For a target fluid the proposed model requires

the critical parameters T_c and P_c , a single saturated liquid TC value, and the dilute-gas term $\lambda_0(T)$, and it can be consequently considered as *semi-predictive*.

The initial improvement of the present model consists in adopting a simple CS format model for the excess TC term, based on high accuracy dedicated equations with a wide range of validity. Since the model is developed using reduced variables, it enables, on one hand, to transfer the performances of the reference fluid equations to the target fluids and, on the other hand, to be applied over a complete λTP surface, excluding a region close to the critical point. Due to its CS structure, the model attains successful results when applied to specific family of homologous fluids. It has been accordingly applied to both HAs and As. The range of validity of the model is limited by the ranges of validity of the dedicated equations adopted for the reference fluids, *methane* and *R134a*. As a consequence, only experimental data included in these ranges have been selected for model validation. For the HAs, based on a total of 3332 points the model gives an AAD of 3.67%, whereas for 354 points of As the corresponding value is 2.87%. Considering that no preliminary data screening has been performed and that the model accuracy is comparable with the uncertainty claimed by the measurements, the present model can be regarded as a valuable application extending the potential of the CS analysis to TC.

REFERENCES

1. G. Cristofoli, M. Grigante, and G. Scalabrin, *Fluid Phase Equilib.* **170**:23 (2000).
2. G. Scalabrin, G. Cristofoli, and M. Grigante, *Int. J. Energy Res.* **26**:1 (2002).
3. U. Gross, Y. W. Song, and E. Hahne, *Int. J. Thermophys.* **13**:957 (1992).
4. U. Hammerschmidt, in *Proc. 12th Symp. Thermophys. Prop.* (Boulder, Colorado, USA, June 19–24, 1994).
5. R. G. Richard and R. I. Shankland, *Int. J. Thermophys.* **10**:673 (1989).
6. O. B. Tsvetkov, Y. Laptev, and A. Asambaev, *Int. J. Thermophys.* **15**:203 (1994).
7. Y. Tanaka, A. Miyake, H. Kashiwagi, and T. Makita, *Int. J. Thermophys.* **9**:465 (1988).
8. J. M. Yin, J. X. Guo, Z. Y. Zhao, L. C. Tan, and M. Zhao, *Fluid Phase Equilib.* **80**:297 (1992).
9. R. A. Perkins, A. Laesecke, and C. A. Nieto de Castro, *Fluid Phase Equilib.* **80**:275 (1992).
10. T. Sousa, P. S. Fialho, C. A. Nieto de Castro, R. Tufeu, and B. Le Neindre, *Int. J. Thermophys.* **13**:383 (1992).
11. B. Le Neindre, Y. Garrabos, A. Sabirzianov, and F. Goumerov, *J. Chem. Eng. Data* **46**:193 (2001).
12. Y. Tanaka, M. Nakata, and T. Makita, *Int. J. Thermophys.* **12**:949 (1991).
13. A. B. Donaldson, *Ind. Eng. Chem.* **14**:325 (1975).
14. T. Makita, Y. Tanaka, Y. Morimoto, M. Noguchi, and H. Kubota, *Int. J. Thermophys.* **2**:249 (1981).

15. K. Stephan and J. Biermann, in *Proc. Int. Refrig. Conf.* (Purdue Univ., West Lafayette, Indiana, 1992).
16. O. B. Tsvetkov and Y. A. Laptev, in *Proc. 8th Symp. Thermophys. Prop.* (Gaithersburg, Maryland, 1981), pp. 396–401.
17. V. Z. Geller, B. Bivens, and A. Yokozeki, in *Proc. 20th Int. Congr. Refrig. IIR* (Sydney, Australia, 1999).
18. J. Yata, M. Hori, T. Hagiwara, and T. Minamiyama, *Fluid Phase Equilib.* **125**:267 (1996).
19. J. C. Nieuwoudt, B. Le Neindre, R. Tufeu, and J. V. Sengers, *J. Chem. Eng. Data* **32**:1 (1987).
20. S. Matsuo, Y. Tanaka, N. Takada, H. Yamamoto, and A. Sekiya, *J. Chem. Eng. Data* **43**:473 (1998).
21. J. Yata, T. Minamiyama, and S. Tanaka, *Int. J. Thermophys.* **5**:209 (1984).
22. M. J. Assael and L. Karagiannidis, *Int. J. Thermophys.* **16**:851 (1995).
23. T. Heinemann, W. Klaen, R. Yourd, and R. Dohrn, *J. Cell. Plastics* **36**:45 (2000).
24. J. Yata, M. Hori, M. Niki, Y. Isono, and Y. Yanagitani, *Fluid Phase Equilib.* **174**:221 (2000).
25. J. V. Widiatmo, T. Tsuge, and K. Watanabe, *J. Chem. Eng. Data* **46**:1442 (2001).
26. D. G. Friend and H. M. Roder, *Int. J. Thermophys.* **8**:13 (1987).
27. R. Krauss, J. Luettmmer-Strathmann, J. V. Sengers, and K. Stephan, *Int. J. Thermophys.* **14**:951 (1993).
28. J. M. Lenoir and E. W. Comings, *Chem. Eng. Progr.* **47**:223 (1951).
29. H. M. Roder, *Int. J. Thermophys.* **6**:119 (1985).
30. H. L. Johnston and E. R. Grilly, *J. Chem. Phys.* **14**:233 (1946).
31. F. G. Keyes, *Trans. ASME* **75**:809 (1954).
32. J. M. Lenoir, W. A. Junk, and E. W. Comings, *Chem. Eng. Progr.* **49**:539 (1953).
33. B. Le Neindre, R. Tufeu, P. Bury, P. Johannin, and B. Vodar, in *Proc. 8th Conf. on Therm. Conductivity*, C. Y. Ho and R. E. Taylor, eds. (Plenum Press, New York, 1969), pp. 229–249.
34. L. T. Carmichael, H. H. Reamer, and B. H. Sage, *J. Chem. Eng. Data* **11**:52 (1966).
35. R. A. Perkins, A. Laesecke, J. Howley, M. L. V. Ramires, A. N. Gurova, and L. Cusco, *NISTIR 6605* (2000).
36. B. Le Neindre and Y. Garrabos, *Int. J. Thermophys.* **20**:375 (1999).
37. Y. Ueno, Y. Nagasaka, and A. Nagashima, in *Proc. 20th Jap. Symp. Thermophys. Prop.* (Kyoto, Japan, 1991), pp. 225–228.
38. M. J. Assael, N. Malamataris, and L. Karagiannidis, *Int. J. Thermophys.* **18**:341 (1997).
39. U. Hammerschmidt, *Int. J. Thermophys.* **16**:1203 (1995).
40. B. Le Neindre and Y. Garrabos, in *Proc. 13th Symp. Thermophys. Prop.* (Boulder, Colorado, 1997).
41. J. Soldner and K. Stephan, *Chem. Eng. Process.* **38**:585 (1999).
42. O. B. Tsvetkov, Y. A. Laptev, and A. G. Asambaev, *Int. J. Refrig.* **18**:373 (1995).
43. R. Afshar and S. C. Saxena, *Int. J. Thermophys.* **1**:51 (1980).
44. Y. Ueno, Y. Kobayashi, Y. Nagasaka, and A. Nagashima, *Nihon Kikai Gakkai Ronbunshu B* **57**:309 (1991).
45. U. Gross, Y. W. Song, J. Kallweit, and E. Hahne, in *Proc. Int. Conf. I.I.R.* (Comm. B1, Herzlia, Israel, 1990/1).
46. R. Yamamoto, S. Matsuo, and Y. Tanaka, *Int. J. Thermophys.* **14**:79 (1993).
47. M. J. Assael and L. Karagiannidis, *Int. J. Thermophys.* **14**:183 (1993).
48. A. N. Gurova, U. V. Mardolcar, and C. Nieto de Castro, in *Proc. 4th Asian Thermophys. Prop. Conf.* (Tokyo, 1995), pp. 129–132.
49. R. Perkins, L. Cusco, J. Howley, A. Laesecke, S. Matthes, and M. L. V. Ramires, *J. Chem. Eng. Data* **46**:428 (2001).

50. A. N. Gurova, U. V. Mardolcar, and C. A. Nieto de Castro, *Int. J. Thermophys.* **20**:63 (1999).
51. A. Grebenkov, Y. G. Kotelevsky, V. V. Saplitza, O. V. Beljaeva, T. A. Zajatz, and B.D. Timofeev, in *Proc. Int. Conf. I.I.R. "CFCs. The day after"* (Padova, Italy, 1994), pp. 419–429.
52. S. H. Kim, D. S. Kim, M. S. Kim, and S. T. Ro, *Int. J. Thermophys.* **14**:937 (1993).
53. O. B. Tsvetkov, Y. A. Laptev, and A. J. Asambaev, *Int. J. Thermophys.* **17**:597 (1996).
54. J. Yata, M. Hori, T. Kurahashi, and T. Minamiyama, *Fluid Phase Equilib.* **80**:287 (1992).
55. A. N. Gurova, U. V. Mardolcar, and C. A. Nieto de Castro, *Int. J. Thermophys.* **20**:63 (1999).
56. S. H. Lee, M. S. Kim, and S. T. Ro, *J. Chem. Eng. Data* **46**:1013 (2001).
57. M. J. Assael, L. Karagiannidis, and W. A. Wakeham, in *ASME Paper 93-WA/HT-26* (ASME Winter Annual Meeting, New Orleans, Louisiana, 1993).
58. B. Le Neindre and Y. Garrabos, *High Temp.-High Press.* **34**:307 (2002).
59. K. Kraft and A. Leipertz, *Int. J. Thermophys.* **15**:791 (1994).
60. J. Yata, T. Kurahashi, and T. Minamiyama, *Fluid Phase Equilib.* **80**:287 (1992).
61. J. Yata, T. Minamiyama, and S. Tanaka, *Int. J. Thermophys.* **5**:209 (1984).
62. M. Papadaki, M. Schmitt, A. Seitz, K. Stephan, B. Taxis, and W. A. Wakeham, *Int. J. Thermophys.* **14**:173 (1993).
63. B. Le Neindre and Y. Garrabos, M. S. Kim, *Int. J. Thermophys.* **22**:723 (2001).
64. A. P. Froba, S. Will, and A. Leipertz, *Int. J. Thermophys.* **22**:1021 (2001).
65. O. B. Tsvetkov and Y. A. Laptev, in *Proc. 5th Asian Thermophys. Prop. Conf.* (Seoul, Korea, 1998), pp. 435–437.
66. U. Gross and Y. W. Song, *Int. J. Thermophys.* **17**:607 (1996).
67. S. U. Jeong, M. S. Kim, and S. T. Ro, *Int. J. Thermophys.* **20**:55 (1999).
68. Y. Yata, M. Hori, K. Kobayashi, and T. Minamiyama, *Int. J. Thermophys.* **17**:561 (1996).
69. M. Papadaki and W. A. Wakeham, *Int. J. Thermophys.* **14**:1215 (1993).
70. Y. Tanaka, S. Matsuo, and S. Taya, *Int. J. Thermophys.* **16**:121 (1995).
71. L. C. Wilson, W. V. Wilding, G. M. Wilson, R. L. Rowley, V. M. Felix, and T. Chilsolm-Carter, *Fluid Phase Equilib.* **80**:167 (1992).
72. L. Q. Sun, M. S. Zhu, L. Z. Han, and Z. Z. Lin, *J. Chem. Eng. Data* **42**:179 (1997).
73. B. Le Neindre and Y. Garrabos, *Int. J. Thermophys.* **22**:701 (2001).
74. S. Matsuo, Y. Tanaka, and T. Sotani, *Fluid Phase Equilib.* **194–197**:1205 (2002).
75. L. T. Carmichael, V. Berry, and B. H. Sage, *J. Chem. Eng. Data* **8**:281 (1963).
76. R. Moster, H. R. Van der Berg, and P. S. Van der Gulik, *J. Chem. Phys.* **92**:5454 (1990).
77. J. M. Lenoir and E. W. Comings, *Ind. Eng. Chem.* **49**:2042 (1957).
78. H. M. Roder, *NBSIR 84–3006* (1984).
79. L. T. Carmichael, J. Jacobsen, and H. Sage, *J. Chem. Eng. Data* **13**:40 (1968).
80. D. E. Leng and E. W. Comings, *Ind. Eng. Chem.* **49**:2042 (1957).
81. H. M. Roder and C. A. Nieto de Castro, *J. Chem. Eng. Data* **27**:12 (1982).
82. J. Yata, M. Hori, T. Hagiwara, and T. Minamiyama, *Fluid Phase Equilib.* **125**:267 (1996).
83. W. J. S. Smith, L. D. Durbin, and R. Kobayashi, *J. Chem. Eng. Data* **5**:316 (1960).
84. V. P. Brykov, G. K. Mukhamedzyanov, and A. G. Usmanov, *J. Eng. Phys. (USSR)* **18**:62 (1970).
85. L. T. Carmichael and H. Sage, *J. Chem. Eng. Data* **9**:511 (1964).
86. W. J. S. Smith, L. D. Durbin, and R. Kobayashi, *J. Chem. Eng. Data* **5**:316 (1960).
87. R. Kandiyoti, E. McLaughlin, and J. F. T. Pittman, *J. Chem. Soc. Faraday Trans.* **68**:860 (1972).